Journal of Autoimmunity 96 (2019) 74–85

Contents lists available at ScienceDirect

Journal of Autoimmunity

journal homepage: www.elsevier.com/locate/jautimm

CRL4^{DCAF2} is required for mature T-cell expansion via Aurora B-regulated proteasome activity

Keqi Fan[a,1], Fei Wang[a,1], Yiyuan Li[a], Lu Chen[a], Zhengjun Gao[a], Yu Zhang[b], Jin-yuan Duan[a], Tao Huang[a], Jiangyan Zhong[a], Rong-bei Liu[b], Xintao Mao[a], Hengyu Fan[a], Xing Guo[a,**], Jin Jin[a,c,*]

[a] Life Sciences Institute, Zhejiang University, Hangzhou, 310058, China
[b] Sir Run Run Shaw Hospital, College of Medicine Zhejiang University, Hangzhou, 310016, China
[c] Key Laboratory of Animal Virology of Ministry of Agriculture, Zhejiang University, Hangzhou, 310058, PR China

ARTICLE INFO

Keywords:
CRL4^{DCAF2}
Cell cycle
Aurora B
Proteasome activity
H4K20me1

ABSTRACT

The proliferation of T cells in peripheral lymphoid tissues requires T cell receptor (TCR)-mediated cell cycle entry. However, the underlying mechanism regulating cell cycle progression in mature T cells is incompletely understood. Here, we have identified an E3 ubiquitin ligase, CRL4^{DCAF2}, as a critical mediator controlling M phase exit in activated T cells. DCAF2 expression is induced upon TCR stimulation and its deficiency attenuates T cell expansion. Additionally, DCAF2 T cell-specific knockout mice display impaired peripheral T cell maintenance and reduced severity of various autoimmune diseases. Continuous H4K20me1 modification caused by DCAF2 deficiency inhibits the induction of *Aurkb* expression, which regulates 26S proteasome activity during G2/M phase. CRL4^{DCAF2} deficiency causes M phase arrest through proteasome-dependent mechanisms in peripheral T cells. Our findings establish DCAF2 as a novel target for T cell-mediated autoimmunity or inflammatory diseases.

1. Introduction

T cells, a type of white blood cells, play a critical role in adaptive immunity against infectious microorganisms and cancer. Hyperactive T cells are also responsible for autoimmune and inflammatory disorders [1]. Upon stimulation by self-antigens, deregulated T cells are activated to enter the cell cycle and proliferate. These deregulated T cells subsequently secrete various effecter cytokines to drive autoimmunity [2]. Consistent with the expansion of other eukaryotic cells, T cell expansion is also tightly controlled by multiple regulatory checkpoints throughout the cell cycle [3]. Entry into the cell cycle is a complex process controlled by the ordered expression and activation of various molecules, including cyclins and cyclin-dependent kinases (CDKs), and the phosphorylation of downstream substrates [4]. Once the signals that trigger the cell cycle are deregulated, immunological tolerance becomes disrupted, and this results in autoimmune responses [5,6]. Nonetheless, the coordinated mechanism of T cell receptor (TCR)-mediated cell cycle regulation remains incompletely investigated.

Current understanding reveal that the first checkpoint controls the transition of eukaryotic cells from the G1 phase into S phase and initiates DNA synthesis [7]. An active complex including Aurora, Survivin, mTOR, p70S6k and 4E-BP1 controls cell cycle progression at the G1/S phase transition [8]. The process of cell cycle in T cells is also tightly controlled by the action of several negative regulators, such as p21, p27, and p53 [9–13]. However, whether these molecules are also involved in the cycling of T cells and their negatively regulatory mechanisms remain controversial.

Ubiquitination is a critical post-translational modification that regulates T cell activation and cell cycle entry [14]. Various E3 ubiquitin ligases and deubiquitinases (DUBs), including Pellino 1, Itch, c-Cbl, Cbl-b, GRAIL, and OTUD7B, have been identified to negatively regulate TCR-CD28 signal transduction and prevent T cell-mediated autoimmune disease progression [15–19]. Ubiquitination also regulates cell cycle in T cells by controlling CDKs and their inhibitors (CDKIs). Mule-deficient mice develop severe experimental autoimmune encephalomyelitis (EAE) and show impaired antiviral immune responses by regulating Krüppel-like factor 4 (KLF4) stability, which is required for the entry of T cells into S phase [20]. Previous studies have shown that cullin ring-finger ubiquitin ligase-4 (CRL4) have multiple functions in maintaining cell cycle progression. CRL4 plays its physiological role

* Corresponding author. Life Sciences Institute, Zhejiang University, Hangzhou, 310058, China.
** Corresponding author.
E-mail addresses: xguo@zju.edu.cn (X. Guo), jjin4@zju.edu.cn (J. Jin).
[1] These authors contributed equally to this work.

https://doi.org/10.1016/j.jaut.2018.08.006
Received 5 July 2018; Received in revised form 18 August 2018; Accepted 21 August 2018
Available online 21 September 2018

by employing more than 90 DDB1-cullin 4-associated factors (DCAFs). Current evidence reveals that $CRL4^{DCAF1}$ is involved in critical steps towards aberrant T cell expansion. $CRL4^{DCAF1}$ promotes the destabilization of p53, which suppresses metabolism and cell cycle entry [21]. However, there is limited evidence regarding the physiological functions of other DCAFs in primary T cells.

In this study, we identified DCAF2 as an essential component of T cell proliferation and T cell-mediated autoimmune responses. $CRL4^{DCAF2}$ has been considered to induce the degradation of p21, SETD8 and Checkpoint kinase 1 (CHK1) by a ubiquitin-dependent mechanism and to promote cell cycle progression [22–24]. Despite extensive *in vitro* studies, the *in vivo* biological functions of $CRL4^{DCAF2}$ have remained largely unknown due to the embryonic lethality of the conventional DCAF2 knockout (KO) mice. Therefore, to clarify the function of $CRL4^{DCAF2}$ in T cell-mediated inflammation, we generated mice specific knockout DCAF2 in T cells for this study. Our studies led to the discovery of a central role for $CRL4^{DCAF2}$ in the control of T cell proliferation and M phase exit. DCAF2 T cell-specific KO mice displayed impaired expansion of peripheral T cells coupled with a reduction in autoimmune symptoms. High-throughput RNA sequencing indicated that the loss of DCAF2 disrupted Aurora B induction and cause M phase arrest. Interestingly, we found that Aurora B physically interacted with the 26S proteasome and regulated proteasome activity, which is important for G2/M phase transition. By chromatin immunoprecipitation sequencing (CHIP-seq) assays, we further demonstrated that DCAF2 depletion attenuated *Aurka* and *Aurkb* induction by enhancing the H4K20me1 modification at their promoters. Therefore, our findings establish $CRL4^{DCAF2}$ as a critical regulator of cell cycle progression in mature T cells and suggest DCAF2 as a therapeutic target for T cell-mediated autoimmune diseases.

2. Results

2.1. TCR triggered DCAF2 induction

To evaluate the potential role of $CRL4^{DCAF2}$ in inflammatory disease, we first analyzed DCAF2 expression in peripheral blood mononuclear cells (PBMCs) from patients with inflammatory bowel disease (IBD). Compared with that in healthy controls, DCAF2 mRNA level was clearly increased in PBMCs from Crohn's disease (CD) or ulcerative colitis (UC) (Fig. 1a). The hallmark of IBD is an aberrant mucosal infiltration by innate immune cells and adaptive immune cells including effector T cells. Although the frequency of total $CD4^+$ T cells in peripheral blood of CD patients were comparable to healthy donors (Supplementary Fig. 1a), the proportion of effector T cells were significantly increased under inflammatory condition (Supplementary Fig. 1b). After isolating different population of T cells from peripheral blood, qPCR assay revealed a significant increment of DCAF2 mRNA level in effector T cells from CD patients, but reduction in non-T lymphocytes (Fig. 1b).

To assess the physiological function of $CRL4^{DCAF2}$ *in vivo*, we next analyzed its expression in different mouse tissues. The mRNA level of DCAF2 was highly expressed in tissues of the immune system including bone marrow (BM), spleen and thymus (Fig. 1c). The abundance analyses also revealed that higher DCAF2 levels were detected in memory T cells than that in naïve T cells (Fig. 1d). Interestingly, we also found a higher mRNA level of *Dcaf2* in Thymus double negative population. As known, thymocytes undergo massive proliferation before T cell receptor (TCR) gene rearrangement, which ensuring the diversification of the TCR repertoire. Thus we proposed that the survival of activated pre-T cells induced by pre-TCR signaling also required DCAF2 expression. However, this conclusion need to be further investigated. To clarify the association of DCAF2 expression with T cell activation, we stimulated naïve $CD4^+$ and $CD8^+$ T cells with anti-CD3 plus anti-CD28 antibodies. We observed a rapid elevation of DCAF2 expression both at mRNA (Fig. 1e) and protein (Fig. 1f) levels in response to TCR engagement. Using PI staining, we analyzed the DCAF2 expression in activated T cells at distinct phases of cell cycle. Notably, elevated DCAF2 level was initiated from S to G2/M phase, suggesting that DCAF2 might play a critical role in late S phase or G2/M phase transition (Fig. 1g–h). All of these data implies that DCAF2 expression is highly correlated with activated T cells and is potentially associated with cell cycle regulation.

2.2. DCAF2 deficiency attenuates T cell-mediated autoimmune diseases

To clarify the pivotal function of $CRL4^{DCAF2}$ in T cells, we crossed $Dcaf2^{flox}$ mice with *Cd4*-Cre mice to generate DCAF2 T cell-conditional KO (TKO) mice (Supplementary Figs. 2a–b). Immunoblotting (IB) analyses revealed a selective defect of DCAF2 in T cells isolated from TKO mice (Supplementary Fig. 2c). TKO mice were born at the expected Mendelian ratio and had grossly normal survival as the WT control mice (data not shown). Surprisingly, loss of DCAF2 completely attenuated all the polarization of naïve $CD4^+$ T cells (Fig. 2a–b), suggesting that $CRL4^{DCAF2}$ may be involved in physiological function of T cells in immune responses. To further evaluate its *in vivo* role, we employed a T cell-dependent autoimmune disease model, EAE, which mimics the human neuroinflammatory disease multiple sclerosis (MS). We immunized WT and TKO mice with a myelin oligodendrocyte glycoprotein (MOG) peptide ($MOG_{35–55}$) plus pertussis toxin. Compared to the WT littermate, TKO mice were refractory to EAE with significantly delayed onset as well as a substantially reduced level of central nervous system (CNS) infiltration (Fig. 2c–d). Flow cytometry analyses revealed that the mononuclear cells in the CNS of TKO mice contained a substantially low percentage of $CD4^+$ and $CD8^+$ T cells and a concomitantly high percentage of CNS-resident microglial cells ($CD11b^+CD45^{mid}$) (Fig. 2e–f). Within the CNS-infiltrating $CD4^+$ T cell population, the numbers of IL-17^+ T helper (Th)-17 cells and IFN-γ^+ Th1 cells was also reduced in the TKO mice (Fig. 2g–h). Upon response to myelin oligodendrocyte glycoprotein (MOG) peptide, DCAF2-deficient T cells had profound defect in recall response, while the WT T cells underwent robust expansion (Fig. 2i). Consistently, peripheral T cells of TKO mice with EAE had a reduced induction of inflammatory cytokines upon *in vitro* restimulation with the MOG peptide (Fig. 2j). Therefore, $CRL4^{DCAF2}$ is essential for autoreactive T cell-mediated EAE pathogenesis.

As elevated level of DCAF2 was observed in $CD4^+$ T cells of IBD patients, we further used a T-cell adoptively transfer model to evaluate the function of $CRL4^{DCAF2}$ on colitis onset. The transfer of naïve $CD45RB^{hi}$ $CD4^+$ T cells from WT mice into *Rag1*-KO mice induced overt colon inflammation associated with body weight loss. However, the transfer of DCAF2-deficient T cells had no effect on body weight (Fig. 2k) or hyperplasia of the colonic mucosa (Fig. 2l–m). Additionally, reduced mRNA levels of IFN-γ and IL-17A were detected in the inflamed area of the colon (Fig. 2n). Collectively, these results suggest that $CRL4^{DCAF2}$ is necessary for T cell-mediated inflammation and autoimmune diseases.

2.3. DCAF2 is required for peripheral T-cell maintenance

As reduced symptom of autoimmune diseases in TKO mice, we next evaluated the development and maintenance of DCAF2-deficient T cells. Compared to WT littermates, TKO mice had a considerably reduced cellularity of the spleen and peripheral lymphoid organs (Supplementary Fig. 2d). Fluorescence-activated cell sorting (FACS) analyses further revealed that this reduction was due to the impaired frequency and total number of mature $CD4^+$ and $CD8^+$ T cells (Fig. 3a–b). Other immune cells such as neutrophil, macrophage and dendritic cells did not contribute to this phenotype (Supplementary Fig. 2e). Although TKO mice also displayed a similar defect in regulatory T (Treg) cells, the proportion of peripheral $\gamma\delta$ T cells was significantly increased (Fig. 3c–d), indicating that $\gamma\delta$ T cells may require different cell cycle regulators from conventional $\alpha\beta$ T cells. FACS analysis further revealed that the reduction of peripheral T cells was not

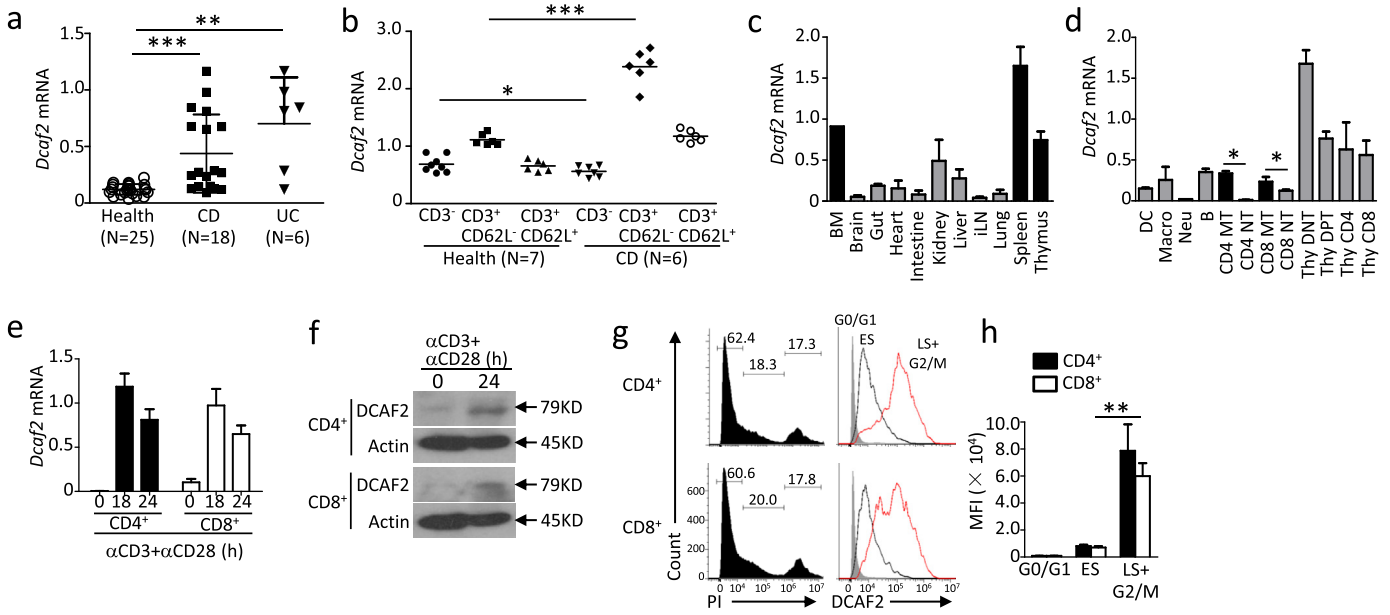

Fig. 1. DCAF2 induction is associated with T cells activation. (**a-b**) qRT-PCR analysis of DCAF2 mRNA level in total PBMCs (**a**) and subpopulation of immune cells as indicated (**b**) from healthy controls, CD and UC patients. (**c-d**) qRT-PCR analyses of *Dcaf2* mRNA level in various tissues (**c**) and immune cells in wild-type mice (**d**). (**e-f**) Naive T cells ($CD44^{lo}CD62L^{hi}$) were isolated from WT mice by FACS sorter, and stimulated with αCD3/αCD28 for indicated time points. The expression of DCAF2 was monitored by qRT-PCR (**e**) and immunoblotting (**f**). (**g-h**) The activated T cells in different cell cycles were gated based on DNA abundance. DCAF2 expression was detected with intracellular staining (**g**) and median fluorescent intensity (**h**). ES means early stage of S phage; LS means late stage of S phage. Data are representative of three independent experiments. All qPCR data are presented as fold relative to the *Actb* mRNA level, and normalized by Bio-Rad CFX Manager 3.1. All data are representative of three independent experiments for each analysis at least. Error bars show mean ± SEM. Significance was determined by two-tailed Student's *t*-test. *P < 0.05; **P < 0.01; *** < 0.005.

due to a defect in thymocyte development, because TKO mice had similar frequencies of double-positive (DP) or $CD4^+$ or $CD8^+$ single-positive (SP) thymocytes as their WT littermates (Fig. 3e–f). Additionally, DCAF2 deficiency did not affect the frequency of T cells at the double negative (DN) stages DN1–DN4 (Fig. 3g). To assess the role of $CRL4^{DCAF2}$ in T cell homeostasis, we measured the frequency of naïve and memory-like T cells in WT and TKO mice. Young adult TKO (6–8 weeks) mice had a significantly reduced frequency of memory-like CD4 T cells and, conversely, an increased frequency of memory-like CD8 T cells (Supplementary Fig. 2f). Collectively, these results suggested that $CRL4^{DCAF2}$ plays a critical role in regulating the survival and homeostasis of peripheral T cells, while $CRL4^{DCAF2}$ is not required for thymocyte development.

To examine whether $CRL4^{DCAF2}$ mediates peripheral T cell maintenance via cell-intrinsic mechanisms, we generated BM chimeric mice by transferring BM cells of TKO mice ($CD45.2^+$), along with those of WT SJL mice ($CD45.1^+$), into lymphocyte-deficient *Rag1* KO mice. The chimeric mice had a similar thymocyte development regarding $CD45.1^+$ and $CD45.2^+$ T cells (Fig. 3h). However, DCAF2-deficient BM cells still yielded a substantially low frequency of mature T cells in the spleen and peripheral lymph nodes (Fig. 3i–k). Furthermore, DCAF2-deficient $CD4^+$ T cells in the chimeras displayed a predominantly effector/memory phenotype and relatively reduced proportion of naïve T cell markers (Supplementary Fig. 2g). All of these data indicated a cell-intrinsic role for $CRL4^{DCAF2}$ in regulating mature T cell maintenance and homeostasis, but not TCR-mediated activation.

2.4. $CRL4^{DCAF2}$ is indispensable for G2/M transition and proliferation of T cells

Due to the reduction of peripheral T cells, we first performed T-cell retention assay to evaluate the capacity of peripheral T cells migration by employing a mixed T-cell transfer approach. We labeled the WT (SJL, $CD45.1^+$) and DCAF2-deficient ($CD45.2^+$) $CD4^+$ T cells with carboxyfluorescein succinimidyl ester (CFSE) fluorescence dyes, and transferred a mixture of the labeled cells (in 1:1 ratio) into *Rag1*-KO mice. After 6 h, we analyzed the distribution of the WT and DCAF2-deficient T cells in the draining lymph nodes and spleen. CFSE intensity implied that no proliferation happened during these 6 h (Supplementary Fig. 3a), but the frequency of $CD45.1^+$ and $CD45.2^+$ cells revealed comparable capacity of retention between WT and DCAF2-deficient T cells (Supplementary Fig. 3b). These results indicate that DCAF2 deficiency did not affect the migration of matured T cells in periphery.

To further examine the physiological function of $CRL4^{DCAF2}$ in T cells, we used CFSE assay to measure T cell proliferation by stimulating naïve $CD4^+$ T cells with agonistic antibodies against TCR (anti-CD3) and CD28 (anti-CD28). DCAF2 deficiency completely abolished proliferation in T cells as revealed by a significant reduction in cell division (assessed by CFSE labeling) relative to than in WT T cell (Fig. 4a–b). The same as $CD4^+$ T cells, DCAF2-deficient $CD8^+$ T cells performed a similar defective proliferation compared to WT control (Supplementary Figs. 4a–b). These data indicated that $CRL4^{DCAF2}$ is required for T cell expansion. BrdU incorporation assays further demonstrated that DCAF2 deficiency caused cell cycle arrest at late stage of S or G2/M phase both *in vivo* (Fig. 4c–d) and *in vitro* (Fig. 4e–f). Consistent with the observation under physiological conditions, TKO mice with EAE also displayed a significant increase in the proportion of draining lymph node (dLN) T cells at late S or G2/M phase (Fig. 4g–h).

To elucidate which signaling pathways were affected by DCAF2 deficiency, we analyzed the majority of differentially expressed genes (DEGs) based on mRNA abundance. As shown in Supplementary Fig. 4c and Supplementary Table 3, we identified 894 DEGs in DCAF2-deficient T cells relative to those in WT T cells. In early stage of TCR-mediated activation, DCAF2 deficiency enhanced T cell responses, suggested by hyperproduction of multiple cytokines. Reversely, DCAF2 deficiency also performed severe suppression of polo-like kinases activity and G2/M DNA damage checkpoint regulation to disrupt the cell cycle progress

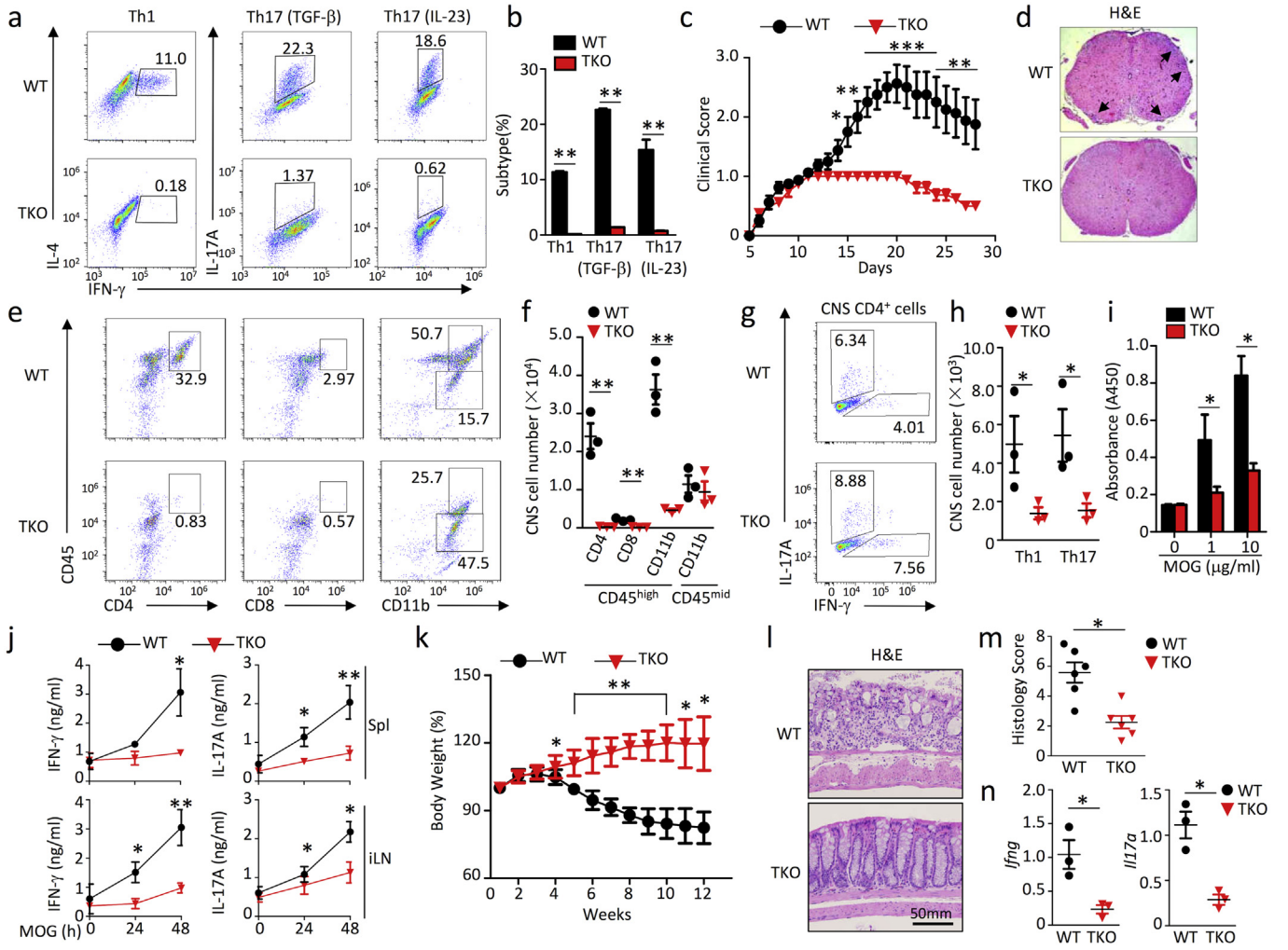

Fig. 2. DCAF2 deficiency restricts T-cell mediated autoimmunity. (**a-b**) Naive CD4$^+$ T cells (CD44^{lo}CD62L^{hi}) from WT and TKO mice were stimulated for 4 days with plate-bound anti-CD3 and anti-CD28 antibodies under different T subpopulation conditions. Frequency of T cell differentiation was analyzed by flow cytometry based on intracellular staining of indicating cytokines. (**c**) Mean clinical scores of WT and TKO mice subjected to MOG35-55-induced EAE (n = 8/group). (**d**) H&E staining of spinal cord sections from WT and TKO EAE mice for visualizing immune cell infiltration (arrows). (**e-f**) Flow cytometry analyses and summary of immune cell infiltration into the CNS (brain and spinal cord) of EAE mice (n = 3, day 14 post-immunization). (**g-h**) Flow cytometry analyses and summary of Th1 and Th17 cells gating with CD4$^+$CD45^{hi} in the CNS, Splenic and draining lymph nodes of EAE mice. (**i**) CCK8 assays of splenic T cells proliferation from day 15 EAE-induced mice, stimulated *in vitro* with the indicated concentrations of MOG-peptide. (**j**) ELISA of the indicated cytokines in supernatants of cultures of splenocytes restimulated for 48 h with MOG peptide (20 μg/ml) *in vitro*. (**k-n**) *Rag1* −/− mice were adoptively transferred with WT or DCAF2-deficient CD4$^+$CD45RB^{hi} T cells (n = 3/group). Bodyweight loss (**k**; percent of starting bodyweight) and colon histology (**l**; H&E staining) were performed as indicated. (**m**) H&E slides of colonic tissue were scored for colitis severity using criteria described in Materials and Methods. (**n**) *Ifng* and *Il17a* induction was determined by qRT-PCR in colonic tissue. All qPCR data are presented as fold relative to the *Actb* mRNA level, and normalized by Bio-Rad CFX Manager 3.1. qPCR Data were normalized to a reference gene, *Actb*. Data shown are representative of three independent experiments. Error bars are mean ± SEM values. *P < 0.05; **P < 0.01; *** < 0.005.

(Fig. 4i). All of these results implied that DCAF2 may have distinct functions in T cells activation and proliferation.

It is known that Cyclin A/CDK2 levels are the highest at the late S-G2 phase of the cell cycle, whereas Cyclin B/CDK1 is mostly induced at the M phase of the cell cycle [25,26]. To clarify which stage was affected by DCAF2 deficiency, we evaluated CDK1/Cyclin B and CDK2/Cyclin A activity in DCAF2-deficient T cells upon TCR/CD28 stimulation. Compared to WT control, DCAF2-deficient T cells displayed significantly enhanced kinase activity of CDK1, but reduced CDK2 activity at 36 h after TCR plus anti-CD28 stimulation, indicating that DCAF2 depletion results in profound M phase arrest in activated T cells (Fig. 4j). DCAF2-deficient CD4$^+$ or CD8$^+$ T cells with abolished mitosis were also more prone to apoptosis than WT cells (Supplementary Figs. 4d–e and Supplementary Figs. 4f–g). These results confirm that the critical role of CRL4^{DCAF2} in activated T cells at M phase exit.

2.5. IL-2 signaling and p53/p21 axis is dispensable for M phase arrest caused by DCAF2 deficiency

The activation of peripheral T cells and cell cycle progression requires signals derived from both the T cell receptor and the IL-2 receptor [27,28]. As shown in Fig. 5a, RNA-seq data revealed that DCAF2 deficiency impaired TCR-mediated IL-2 induction. Parallel QPCR also revealed a profound reduction in IL-2 induction in DCAF2-deficient T cells (Fig. 5b). However, the heatmap indicated that DCAF2 deficiency promoted IL-2 receptor-mediated signaling transduction, suggested by increment of IL-2-targeted genes expression (Fig. 5a). To further clarify the role of IL-2 in DCAF2 deficiency-mediated M phase arrest, we assessed T cell proliferation in the presence of excess IL-2 by CFSE labeling. The results indicated that exogenous IL-2 moderately enhanced the proliferation of WT T cells, but did not restore the defective expansion of DCAF2-depleted T cells (Fig. 5c–d).

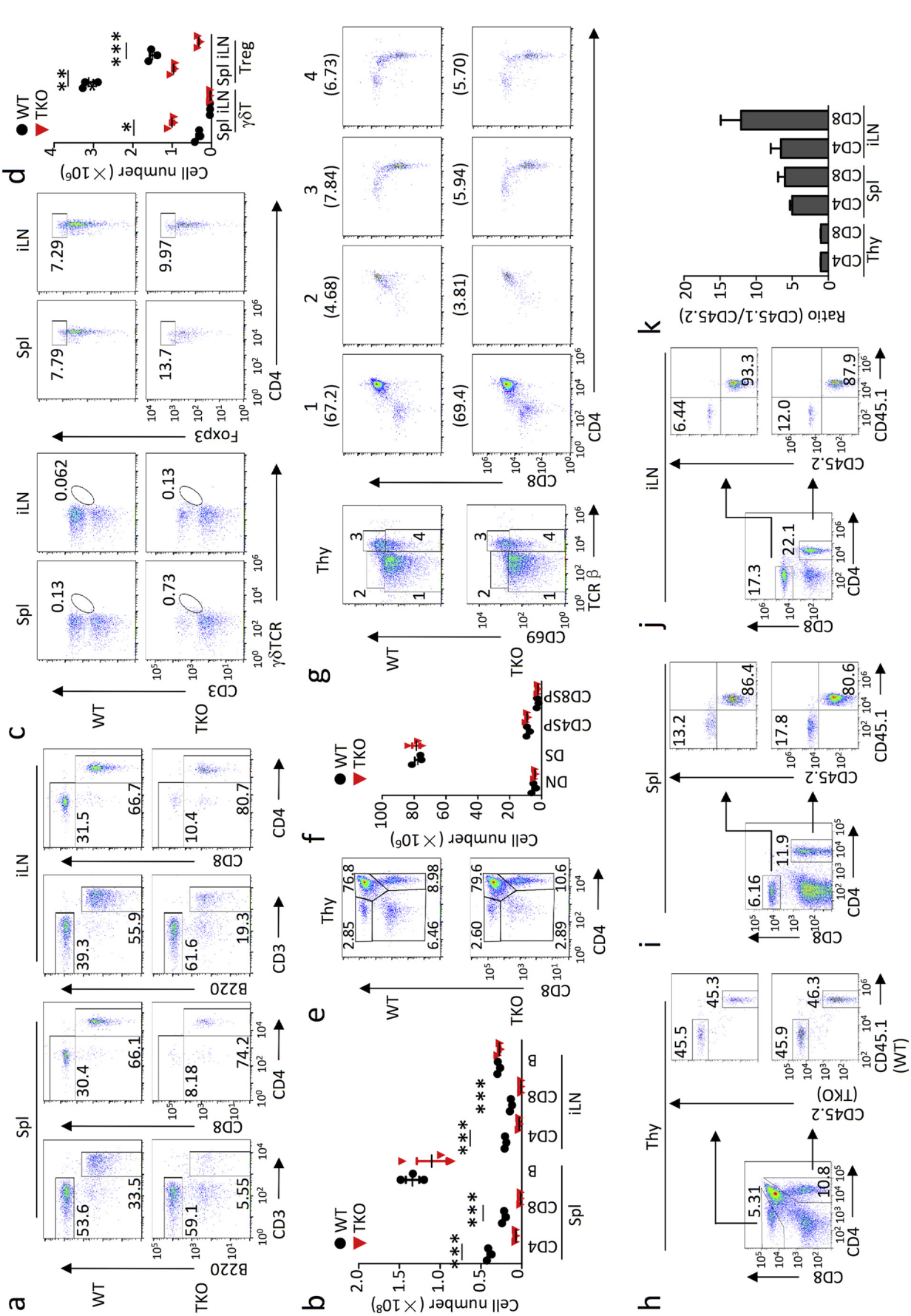

Fig. 3. CRL4^{DCAF2} controls T-cell maintenance, but not development. (**a-b**) Flow cytometric analyses of the frequency and summary graph of CD4$^+$ and CD8$^+$ T cells in splenocytes and iLN. (**c-d**) Representative plot and frequencies of γδT or Treg cells in inguinal lymph node (iLN) and spleen (Spl). (**e-g**) Flow cytometric analyses of the percentage of thymic subpopulations (**e-f**) or the surface expression of CD69 and TCR on thymocytes (**g**) from 6-wk-old WT and TKO mice, presented as a representative FACS plot. (**h-j**) Flow cytometric analysis of total thymocytes (**h**), T cells in spleen (**i**) and iLN (**j**) in *Rag1*-KO recipient mice adoptively transferred with BM cells derived from TKO mice (CD45.2$^+$) along with BM cells derived from B6.SJL mice (CD45.1$^+$). (**k**) The ratio of CD45.1$^+$ to CD45.2$^+$ T cells from the BM chimeric mice described as above. Data are representative of three independent experiments and three mice for each FACS analysis at least. Error bars show mean ± SEM. Significance was determined by two-tailed Student's *t*-test. *P < 0.05; **P < 0.01.

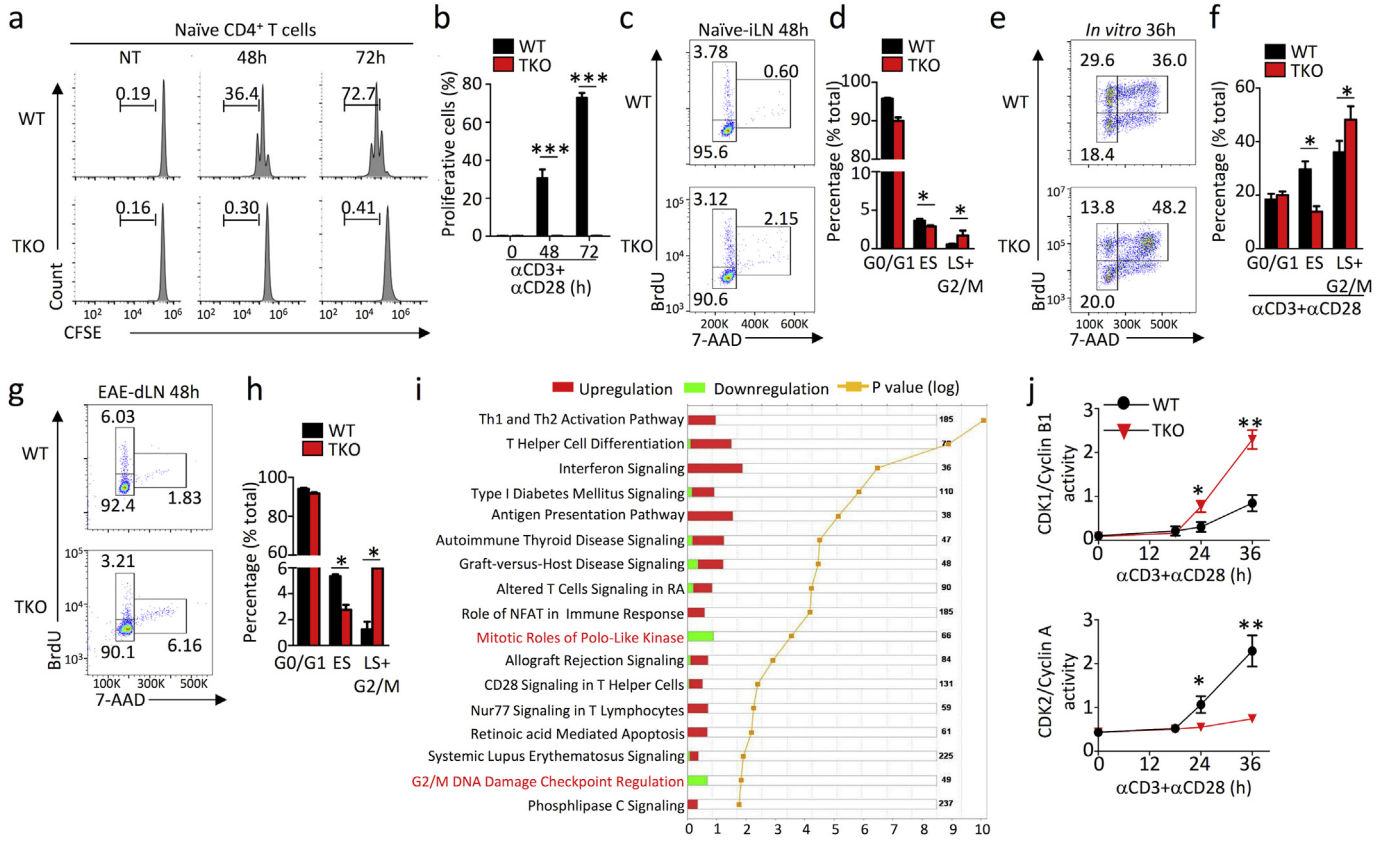

Fig. 4. CRL4^{DCAF2} is critical for T-cell proliferation and M phase exit. (**a**) Naive CD4$^+$ T cells (CD44^{lo}CD62L^{hi}) were isolated from WT and TKO mice. These T cells were labeled with 5 μM CFSE and stimulated with plate-bound anti-CD3 and anti-CD28 antibodies as indicated. Proliferative ratio is assessed as CFSE dilution by FACS. (**b**) The summary of CFSE-labeled T cells proliferation. (**c-f**) Cell cycle processes of T cell from WT and TKO mice were evaluated by the DNA synthesis *in vivo* (**c-d**) and *in vitro* (**e-f**). ES means early stage of S phage; LS means late stage of S phage. (**g-h**) DNA synthesis of CD4$^+$ T cells in draining lymph node (dLN) from WT and TKO mice subjected to MOG35-55-induced EAE. (**i**) Actual numbers of down- and upregulated DEG were shown inside bars. Green bars denoted the percentage of downregulated and red bars performed the percentage of upregulated genes. The yellow line denotes the likelihood [−log (P value)] that the specific pathway was affected by DCAF2 deficiency. (**j**) The CDK1/Cyclin B and CDK2/Cyclin A activities were determined by NADH oxidation activity. All qPCR data are presented as fold relative to the *Actb* mRNA level, and normalized by Bio-Rad CFX Manager 3.1. Data shown are representative of three independent experiments and three mice for each FACS analysis at least. Error bars are mean ± SEM values. *P < 0.05; **P < 0.01; ***P < 0.005. (For interpretation of the references to colour in this figure legend, the reader is referred to the Web version of this article.)

p21 is a potent cyclin-dependent kinase inhibitor (CKI), and functions as a regulator of cell cycle progression at G1 and S phase. As previously reported, p21 plays a critical role in controlling proliferation and homeostasis of effector/memory T cells [12,29]. p21 degradation has been shown to be promoted by CRL4^{DCAF2} ubiquitin ligase in response to low doses of ultraviolet irradiation [24,30]. Therefore, we next investigated whether the defect in T cell maintenance was due to p21 accumulation and subsequent S phase arrest. Compared to WT controls, DCAF2-deficient T cells did not display changes in the mRNA levels of *Cdkn1a* or its upstream inductor *Tp53* (Fig. 5e). Consistent with previous findings, the protein level of p21 was also elevated in DCAF2-deficient T cells (Fig. 5f). To further address the role of the DCAF2–p21 axis in mature T cells, we crossed *Dcaf2*$^{fl/fl}$*Cd4*^{Cre} with *Tp53*$^{fl/fl}$ mice to delete DCAF2 in a p53 KO background. IB analyses revealed that p53 depletion impaired p21 induction both in WT and DCAF2 KO T cells (Fig. 5f). Although DCAF2 KO mice in a p53-deficient background exhibited largely normal T cell development in the thymus, they remained impairment of mature T cell maintenance in peripheral tissues (Fig. 5g–h). Therefore, TCR-induced p53 and its target p21 are not involved in the M phase arrest of DCAF2 KO T cells.

2.6. DCAF2 deficiency attenuates Aurora B induction via H4K20me1 modification

As previous report, DCAF2 restricts the level of H4K20me1 during mitosis via promoting SETD8 degradation. To clarify the underlying mechanism of DCAF2 regulating T cells expansion, we first evaluated the global level of H4K20me1 in resting and activated CD4$^+$ T cells. The FCAS analysis demonstrated that H4K20me1 in DCAF2-deficient T cells was broadly increased without affecting its distribution after activated by TCR stimulation (Fig. 6a–b). H4K20me1 was known as a repressor for various genes expression during the cell cycle process. Therefore, we evaluated the overlap of H4K20me1-enriched genes with the downregulated genes determined by transcriptome analyses in the absence of DCAF2. Among the identified group of 136 genes, 64 contained H4K20me1 enriched peaks (Fig. 6c and Supplementary Table 4). Among these genes, we identified transcription start sites (TSS) of *Aurka* and *Aurkb* were substantially enriched with H4K20me1 (Fig. 6d). This enrichment of H4K20me1 at *Aurkb* and *Aurka* loci was also validated by ChIP coupled with QPCR assays (Supplementary Fig. 5a).

To assess the role of H4K20me1 in gene induction, we measured Aurora B and Aurora A expression in WT and DCAF2-deficient T cells. Aurora B induction was obviously attenuated both at mRNA (Fig. 6e) and protein levels (Fig. 6f–g) in DCAF2-deficient T cells compare to WT control. It is known that Aurora B regulates cell cycle-associated phosphorylation of chromosomal substrates, such as histone 3 at serine 10 (H3S10) during G2/M phase. Consistent with the reduction in Aurora B expression, phosphorylation of H3S10 was also inhibited by DCAF2 depletion (Fig. 6h–i). To further evaluate the function of Aurora B in M phase, we treated activated WT T cells with an Aurora B

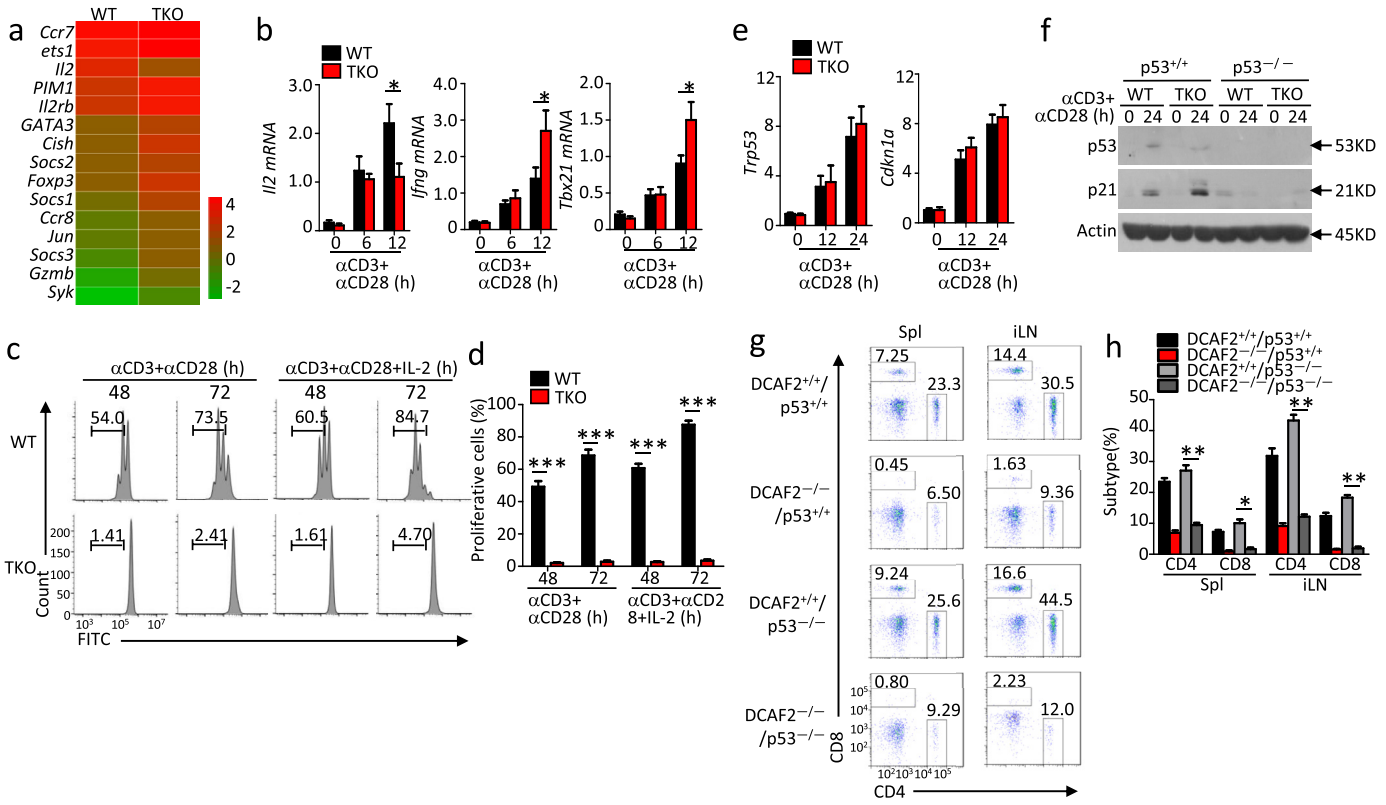

Fig. 5. Neither IL-2 signaling nor p53-p21 axis is dispensable for proliferative defect of DCAF2-deficient T cells. (**a**) Heat map showed the major IL-2 targeted genes in WT and DCAF2-deficient T cells. (**b**) qRT-PCR analysis of *Il2*, *Ifng* and *Tbx21* mRNA (responding to TCR stimuli. (**c-d**) The CFSE assay for proliferative capacity of naïve CD4$^+$ T cells were stimulated with anti-CD3/CD28 plus external IL-2. (**e**) The transcriptional levels of *Tp53* and *Cdkn1a* in WT and DCAF2^{TKO} mice were monitored by qRT-PCR. (**f-h**) TKO mice were bred with *Tp53*^{flox} mice to generate DKO mice. The protein expressions of p53 and p21 were analyzed by immunoblotting (**f**). (**g-h**) The FACS plot and summary of CD4$^+$ and CD8$^+$ T cells in spleen and peripheral lymph nodes from WT and TKO mice in p53 KO background were assessed by flow-cytometry. All qPCR data are presented as fold relative to the *Actb* mRNA level, and normalized by Bio-Rad CFX Manager 3.1. Data are representative of three independent experiments and three mice for each FACS analysis at least. Error bars show mean ± SEM. Significance was determined by two-tailed Student's *t*-test. *P < 0.05; **P < 0.01.

inhibitor, hesperadin for 12 h before harvesting the cells. As shown in Fig. 6j–k, Hesperadin treatment significantly increased the proportion of T cells at G2/M phase. We next reconstituted Aurora B in DCAF2-deficient BM cells, and isolated GFP$^+$ cells by FACS. After mixing 1:1 with SJL BM cells, reconstituted BM cells were transferred into *Rag1*-KO mice. Eight weeks later, the expressive level of reconstituted Aurora B was comparable with WT T cells (Supplementary Fig. 5b). FACS analyses revealed that reconstituted Aurora B partially rescued the defective maintenance of DCAF2 KO T cells (Fig. 6l–m). Taken together, these *in vitro* and *in vivo* results highlight the functional importance of Aurora kinases in CRL4^{DCAF2}-mediated T cell expansion.

2.7. Aurora B-regulating proteasome activity is critical for cell cycle progress

Aurora B is considered a part of centromeres from prometaphase to metaphase and plays an essential role in chromosome segregation [31,32]. Interestingly, Aurora B has been predicted to interact with multiple subunits of the 26S proteasome (Fig. 7a). To confirm this interaction, we performed Co-immunoprecipitation (Co-IP) assays to examine the physically association between Aurora B and the 26S proteasome. Under overexpressed 26S proteasome subunit Rpn1 in 293T (Fig. 7b) or endogenous (Fig. 7c) conditions with subunit Rpn2, Aurora B strongly interacted with 26S proteasome subunits Rpn1/2. Next, using a shRNA approach, we evaluated the role of Aurora B in regulating proteasome activity. Similar to the observations with the positive control Dual-specificity tyrosine-regulated kinase 2 (DYRK2) shRNA [33], silencing of *Aurkb* by three independent shRNAs consistently abolished proteasome activity against Suc-LLVY-AMC (fluorogenic substrate) by approximately 20–30% (Fig. 7d). We further characterized proteasome activity affected by Aurora B directly by an *in vitro* assay. Affinity-purified 26S proteasome treated with endogenous Aurora B isolated from activated WT T cells showed markedly increased peptidase activity towards Suc-LLVY-AMC (Fig. 7e). Unfortunately, we did not observe a similar function of Aurora A in controlling proteasome activation (Fig. 7e).

Consistently, DCAF2 depletion suppressed Aurora B induction, and caused a reduction of endogenous proteasome activity towards a fluorogenic peptide substrate Suc-LLVY-AMC by approximately 15% (Fig. 7f). Reduced proteasome activity increased global K48-linked polyubiquitination in DCAF2-deficient T cells when activated by TCR stimulation (Fig. 7g). To evaluate the role of Aurora B in DCAF2-regulating proteasome activity, we treated WT and DCAf2-deficient T cells with hesperadin. The difference of proteasome activity between WT and DCAF2-deficient CD4$^+$ T cells was significantly erased by hesperadin (Fig. 7h), indicating that Aurora kinases B are required for maintaining proteasome activity. MG132, a proteasome inhibitor is used for inducing cell growth inhibition and restricting cells at G2/M phase progression [34]. After treated with MG132, BrdU assays revealed that WT and DCAF2-deficient T cells performed a comparable accumulation in G2/M phase, indicating DCAF2 deficiency-induced M phase arrest occurs via the regulation of proteasome activity (Fig. 7i–j).

CRL4^{DCAF2} has emerged as a master regulator and disruptor of CDT1 stability that prevents replication [35,36]. Consistent with previous

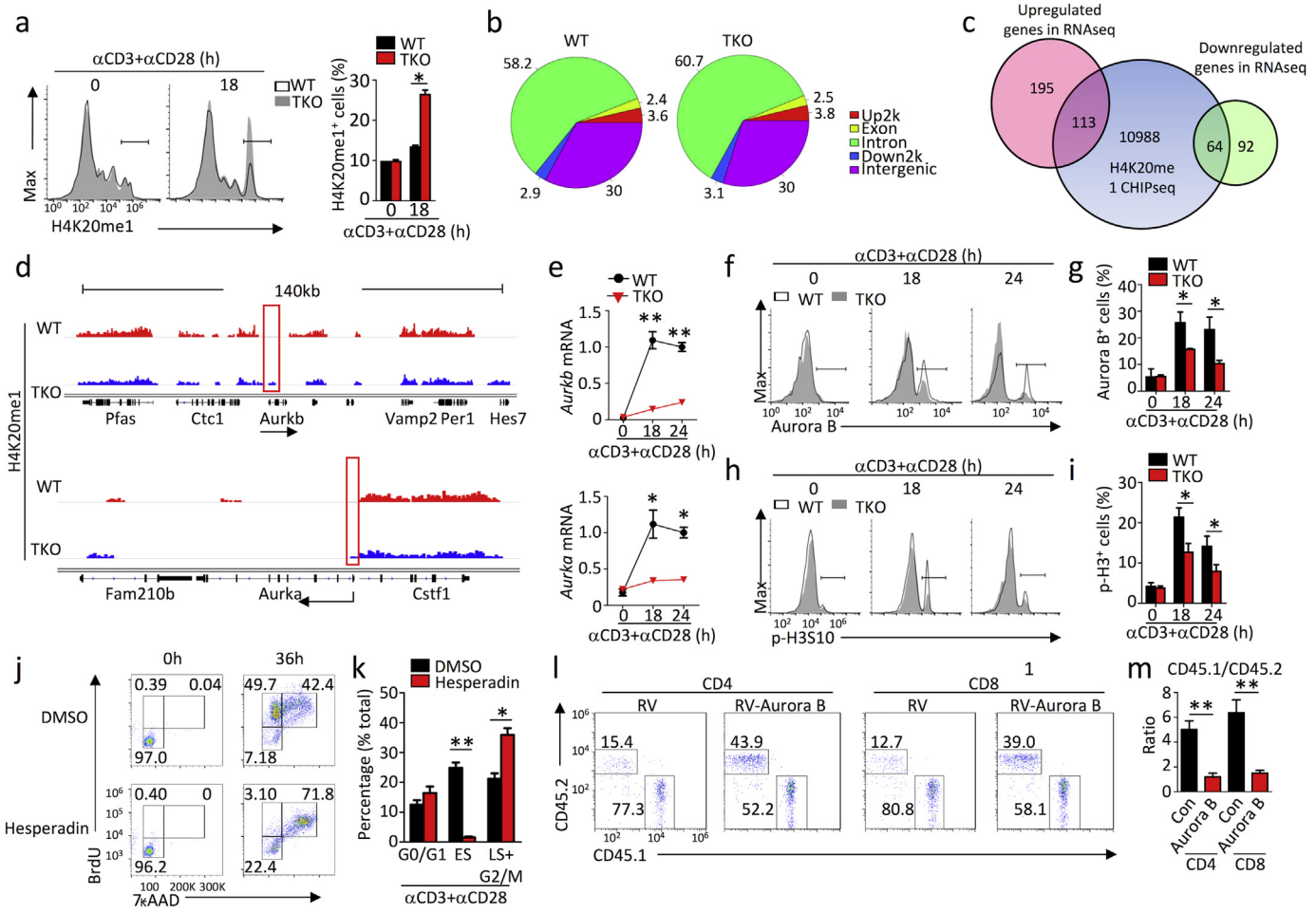

Fig. 6. DCAF2 deficiency restricts Aurora B expression by H4K20me1 modification. (**a**) The broad H4K20me1 level was assessed by flow-cytometry at 18 h after TCR activation. (**b**) The pie chart from WT and DCAF2 KO T cells visualizes the distribution of H4K20me1 peaks over different categories of elements such as promoter, coding exon, and intron. (**c**) Venn diagram showing the numbers of genes harboring H4K20me1 peaks and displaying down- and upregulation in DCAF2 KO T cells. (**d**) Snapshot of the H4K20me1 ChIP-Seq signal at the *Aurkb* and *Aurka* loci in activated T cells from WT and TKO mice. (**e-g**) The level of Aurora A or B in WT and DCAF2 KO T cells was monitored by qRT-PCR (**e**) and intracellular staining by FACS analyses (**f-g**). (**h-i**) The phosphorylated level of H3 at serine 10 was measured by flow-cytometry at 18 and 24 h after TCR activation. (**j-k**) WT T cells were stimulated with anti-CD3 plus anti-CD28 for 36hrs. These T cells were treated with Aurora kinase inhibitor hesperadin for 12hrs before harvested. DNA synthesis and summary were detected with BrdU and 7-AAD staining. (**l-m**) The distribution of $CD4^+$ and $CD8^+$ T populations was detected by FACS in the spleen of the *Rag1*−/− chimeric mice. *Rag1*−/− recipient mice were transferred with $CD45.1^+$ (WT) and $CD45.2^+$ (DCAF2-KO) T cells reconstituted with empty vector or Aurora B (n = 3).All qPCR data are presented as fold relative to the *Actb* mRNA level, and normalized by Bio-Rad CFX Manager 3.1. Data shown are representative of three independent experiments. Error bars are mean ± SEM values. *P < 0.05; **P < 0.01.

observations, DCAF2 deficiency significantly enhanced CDT1 accumulation in response to TCR stimulation (Supplementary Figs. 6a–b). MG132 restored CDT1 expression in WT cells but moderately affected CDT1 expression in DCAF2 KO cells (Supplementary Fig. 6c). Overexpression of CDT1 completely abolished T cell proliferation and mimicked the phenotypes caused by DCAF2 depletion (Supplementary Figs. 6d–e). Surprisingly, ubiquitination assays revealed that DCAF2 deficiency did not affect the polyubiquitinated levels of CDT1 (Supplementary Fig. 6f), indicating that $CRL4^{DCAF2}$ regulated CDT1 stability by regulating proteasome activity but not by directly promoting CDT1 ubiquitination. Together, these data demonstrate that $CRL4^{DCAF2}$ is required for maintaining 26S proteasome activity during the M phase, and thus plays an essential role in controlling cell cycle progression.

3. Discussion

The clonal expansion of antigen-specific T cells is essential for the induction of effective adaptive immune responses. A key process in T cell proliferation is cell cycle entry, which ensures proper cell division. The cycling of T cells is tightly controlled by the ordered expression of cyclin/CDK complexes [4,7]. These kinases undergo periodic proteolysis to maintain the integrity of T cells. Two crucial E3 enzymes are responsible for regulating cell cycle progression and mediating the degradation of key cell cycle proteins [37]. APC/C^{Cdc20} initiates metaphase to anaphase transition, while APC/C^{Cdh1} contributes to transition from M/G1 transition [37]. The Skp1/Cul1/F-box protein (SCF) complex predominantly drives cell cycle progression throughout G1/S transition [7]. Recently, a novel E3 ubiquitin ligase $CRL4^{DCAF2}$ has been characterized as a master regulator that prevents rereplication of DNA in S phase [23,35,36]. $CRL4^{DCAF2}$ promotes the ubiquitin-dependent proteolysis of various substrates such as CDT1, p21, and Set8 [36]. Nonetheless, due to the embryonic lethality of DCAF2 deficiency in mice, whether or how $CRL4^{DCAF2}$ regulates T cell maintenance and the underlying mechanisms remained poorly understood. In this study, we generated mice with conditional KO of DCAF2 in T cells. Our study led to the discovery of a critical function for $CRL4^{DCAF2}$ in T cell maintenance and proliferation. DCAF2 expression is highly associated with T

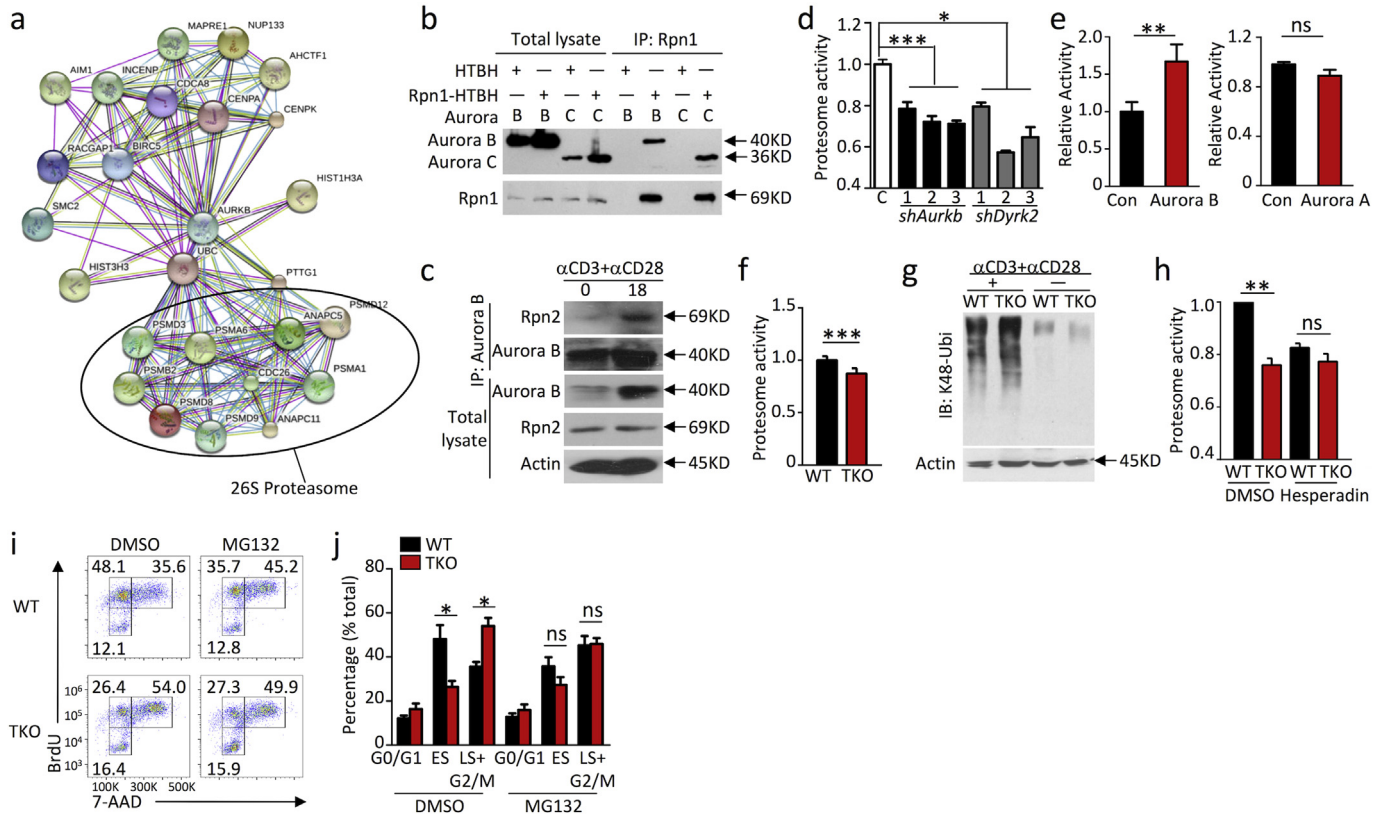

Fig. 7. CRL4^{DCAF2} regulates 26S proteasome activity via Aurora B. (**a**) The protein–protein interaction network of Aurora B was generated using the STRING database (Version 9.1, http://string-db.org/). (**b**) The interaction between Aurora B and 26S proteasome in 293T cells were assessed by co-transfection with indicated genes plasmids. Whole-cell lyses were subjected to IP using anti-Rpn1, followed by IB analyses of the associated FLAG-Aurora using anti-FLAG. (**c**) 18hrs after TCR stimulation, whole-cell lyses were subjected to IP using anti-Aurora B, followed by IB analyses of the associated Rpn2. (**d**) Proteasome activity in total cell lysates from 293T cells transfected with control, *Aurkb* or *Dyrk2* shRNAs was measured using Suc-LLVY-AMC as the substrate. (**e**) 26S proteasomes were purified from 293T cells, and then incubated with pull-down Aurora B or Aurora A *in vitro*. After removal of these Aurora kinases, proteasome activity was measured with Suc-LLVY-AMC. (**f**) Proteasome activity in total cell lysates from WT and DCAF2 KO activated T cells was measured with Suc-LLVY-AMC. (**g**) IB analyses of the total K48-linked polyUbi in naive T cells from WT and TKO mice stimulated with anti-CD3 plus anti-CD28. (**h**) Proteasome activity of activated WT and DCAF2 KO T cells treated with hesperadin for 12 h (**i-j**) WT and DCAF2 KO T cells stimulated with anti-CD3 plus anti-CD28 for 36hrs. These T cells were treated with MG132 2hrs before harvest. Cell cycle processes of these T cell were evaluated by the BrdU plus 7-AAD staining *in vitro*. Data are representative of three independent experiments. Error bars show mean ± SEM. Significance was determined by two-tailed Student's *t*-test. *P < 0.05; **P < 0.01; ***P < 0.005.

cell activation, and DCAF2 restricts H4K20me1 modifications at *Aurk* promoter loci in activated T cells during the M phase. Aurora B has been identified as a pivotal kinase for enhancing 26S proteasome activity, which is indispensable for the CRL4^{DCAF2}-dependent proliferation of T cells. However, the function of CRL4^{DCAF2} in other immune cells remains under investigation.

IL-2 has long been recognized as a major T cell growth factor and a regulator of G1/S phase progression [38,39]. However, current evidence on the potential function of IL-2 in T cells proliferation remains controversial. *In vitro* studies have revealed that IL-2 efficiently enhances the growth of activated T cells [38]. However, using both *in vivo* and *in vitro* assays with γc−/− T cells, another study indicated that the proliferation of naïve CD4$^+$ T cells is independent of IL-2 [40]. RNA-seq analyses indicated that IL-2 induction was severely abolished in DCAF2-deficient T cells. Moreover, exogenous IL-2 could not restore the proliferative capacity of DCAF2-deficient naïve T cells. Together, these results indicated that IL-2 does not contribute to the proliferative defect in DCAF2 KO T cells. However, whether IL-2 is involved in memory T cells differentiation remains to be investigated.

It is known that cell cycle suppressors p21 and p27 abolish TCR-mediated proliferation and activation [12,41,42]. Our study demonstrated that the loss of p53, a p21 inducer, in DCAF2-deficient T cells failed to alleviate M phase arrest and proliferation defect. c-Myc is also important for both T cell growth and proliferation [43]. However, we did not observe any change in c-Myc expression during T cell activation (data not shown). These data suggest that neither p21 nor c-Myc is involved in CRL4^{DCAF2}-mediated T cell expansion and cell cycle progression.

In this study, the Aurora B-phosphorylated 26S proteasome was shown to play an important role in cell cycle regulation. Recently, the 26S proteasome has been shown to be regulated at several levels including transcriptional and post-translational modifications at different cell cycle stages [44–46]. The 26S proteasome contains more than 300 phosphorylation sites that are dynamically regulated during the cell cycle. However, whether and how cell cycle-related kinases affect proteasome activity remains poorly understood. DYRK2 has been identified to phosphorylate Rpt3-Thr25, which contributes to tumor growth [33]. Here, we show that the 26S proteasome is also dynamically phosphorylated by Aurora B in a cell cycle-regulated manner. Silencing of Aurora B in T cells severely impaired 26S proteasome activity and caused M phase arrest. The specific sites phosphorylated by Aurora B and its potential function in proteasome activity need to be further studied. Our findings demonstrate a novel signaling network that regulates primary T cell proliferation and has profound therapeutic implications for T cell-mediated autoimmune diseases.

4. Method

4.1. Mice

Dcaf2$^{fl/fl}$ mice were generated by the Model Animal Resource Information Platform, Model Animal Research Center of Nanjing University. Embryonic stem cells used to generate this mouse strain were purchased from the European Conditional Mouse Mutagenesis Program (ES cell clone EPD0842_C05). The *Dcaf2*-floxed mice were further crossed with *Cd4*-Cre mice (all from Jackson Laboratory, C57BL/6 background) to generate T cell conditional DCAF2 KO (*Dcaf2*$^{f/f}$*Cd4*-Cre, TKO). *Rag1*$^{-/-}$ mice were from Model Animal Research Center of Nanjing University. *Dcaf2*$^{f/f}$*Cd4*-Cre mice were further crossed with *Trp53*$^{f/f}$ mice to generate *Dcaf2*$^{+/+}$*Trp53*$^{+/+}$*Cd4*-Cre (DCAF2$^{+/+}$/p53$^{+/+}$), *Dcaf2*$^{f/f}$*Trp53*$^{+/+}$*Cd4*-Cre (DCAF2$^{-/-}$/p53$^{+/+}$), *Dcaf2*$^{+/+}$*Trp53*$^{f/f}$*Cd4*-Cre (DCAF2$^{+/+}$/p53$^{-/-}$) and *Dcaf2*$^{f/f}$*Trp53*$^{f/f}$*Cd4*-Cre (DCAF2$^{-/-}$/p53$^{-/-}$) mice. Heterozygous mice were bred to generate littermate controls and conditional KO mice for experiments. Outcomes of animal experiments were collected blindly and recorded based on ear-tag numbers of the experimental mice. Mice were maintained in specific pathogen-free facility, and all animal experiments were conducted in accordance with protocols approved by the Institutional Animal Care and Use Committee of Zhejiang University.

4.2. Plasmids, antibodies, and reagents

Antibodies for IKBα (C-21), p65 (C-20), Lamin B (C-20), ERK (K-23), phospho-ERK (E-4), JNK1 (C-17), p38 (H-147), IKKα (H-744), p105/p50 (C-19), Akt1 (B-1), Zap70 (1E7.2), Lck (3A5), PLC-γ (1249) and c-Rel (SC-71), as well as a control rabbit IgG (SC-2027) were from Santa Cruz Biotechnology. Antibodies for phospho-Akt (Ser473; D9E), phospho-IκBα (Ser32; 9241), phospho-JNK (Thr180/Tyr185; 9251), phospho-p38 (Thr180/Tyr182; 9211), phospho-p105 (Ser933), phospho-Lck (2751), phospho-Zap70 (Tyr319; 2701), phospho-PLC-γ (Tyr319) and phospho-IKKα/β (Ser176/180) were purchased from Cell Signaling Technology Inc. Anti-Actin (C-4) was from Sigma. DCAF2 antibody (ab72264), Aurora B antibody (ab2254) and phospho-H3S10 (ab5176) were purchased from Abcam. Fluorescence antibodies for DCAF2, AuroraB, and phospho-H3S10 antibodies were labeled by Lightning-Link Fluorescein Conjugation Kit (Innova Biosciences, 707-0010). Other Fluorescence-labeled antibodies are listed in the section of flow cytometry and cell sorting.

4.3. Flow cytometry, cell sorting, and intracellular staining (ICS)

Spleen or draining lymph node were subjected to flow cytometry using CytoFlex (Beckman Coulter) and the following fluorescence-labeled antibodies from eBioscience: PB-conjugated anti-CD4, and anti-CD11c; PE-conjugated anti-B220 and anti-F4/80; PerCP5.5-conjugated anti-Gr-1 (Ly6G); APC-conjugated anti-CD62L; APC-CY7-conjugated anti-CD11b and anti-CD8; and FITC-conjugated anti-IFNγ, anti-CD44 and anti-Foxp3.

For ICS, T cells were stimulated for 4 h with PMA plus ionomycin in the presence of monensin and then subjected to intracellular IFN-γ and IL-17A by flow cytometry analysis.

4.4. T cell isolation and stimulation

Primary CD4$^+$ T cells were isolated from the spleen and LNs of young adult mice (6–8 wk old) using anti-CD4 magnetic beads. Naïve CD4$^+$ cells were further purified by flow cytometric cell sorting based on CD4$^+$ CD44^{lo}CD62L^{hi} surface markers, respectively. The cells were stimulated with plate-bound anti-CD3 (1 μg/ml) and anti-CD28 (1 μg/ml) in replicate wells of 96-well plates (10^5 cells per well) for ELISA, 12-well plates (10^6 cells per well) for quantitative RT-PCR (qRT-PCR), and 6-well plates (5×10^6 per well) for IB assays. Where indicated, the cells were acutely stimulated using an antibody cross-linking protocol as previously described [47].

4.5. BrdU incorporation assay

In vitro, activated T cells were pulsed with BrdU for 1 h prior to harvest, stained with BrdU staining kit as per manufacture's protocol (BD Pharmingen, 559619) and analyzed by flow-cytometry.

In vivo, WT and DCAF2 TKO mice were injected intravenously injection of 2 mg BrdU in PBS. 24hrs later, different populations of T cells were isolated with autoMACS based on the surface markers, and then stained by using an anti BrdU kit (BD Pharmingen, 559619) according to manufacturers' instructions.

4.6. Bone marrow chimeras

Rag1$-/-$ mice were lethally irradiated (950 rad) and adoptively transferred with WT (CD45.1 SJL) mixed with TKO (CD45.2) bone marrows (1:1) to generate WT and TKO chimeric mice, respectively. After 6 wk, the WT and TKO chimeric mice were analyzed by flow cytometry.

4.7. CD4$^+$ T cell differentiation

Naive CD4$^+$ T cells (CD4$^+$CD44^{lo}CD62L^{hi}) were isolated from spleens and LNs of WT or TKO mice and stimulated with plate-coated anti-CD3 (5 μg/ml) and anti-CD28 (1 μg/ml) under Th1 (10 ng/ml IL-12 and 5 μg/ml anti-IL-4), TGF-β Th17 (1 ng/ml TGF-β 10 ng/ml IL-6, 5 μg/ml anti-IFN-γ, and 5 μg/ml anti-IL-4), IL-1β Th17 (10 ng/ml IL-1β, 10 ng/ml IL-6, 20 ng/ml IL-23, 5 μg/ml anti-IFN-γ, and 5 μg/ml anti-IL-4) or Treg cell (1 ng/ml TGF-β and 10 ng/ml IL-2) conditions. After 4 d of differentiation, cells were subjected to intracellular cytokine staining (ICS) and flow cytometry analyses [47].

4.8. Analysis of apoptosis

Apoptotic T cells were measured based on staining with annexin V and PI. Briefly, the cells were incubated for 0.5 h in a hypotonic PI-staining buffer (0.1% sodium citrate, 0.1% Triton X-100 and 50 μg/ml PI) and then subjected to flow cytometry to quantify the apoptotic/necrotic cell population (sub-G1/G0 cell fraction). Early-stage apoptosis was determined by FITC-annexin V staining (3 μl, BD Biosciences), based on the translocation of phosphatidylserine to the extracellular membrane leaflet in apoptotic cells.

4.9. Induction and assessment of EAE

For active EAE induction, age- and sex-matched mice were immunized s.c. with MOG_{35-55} peptide (300 μg) mixed in CFA (Sigma-Aldrich) containing 5 mg/ml heat-killed *Mycobacterium tuberculosis* H37Ra (Difco). Pertussis toxin (200 ng, List Biological Laboratories) in PBS was administered i.v. on days 0 and 2. Mice were examined daily and scored for disease severity using the standard scale: 0, no clinical signs; 1, limp tail; 2, paraparesis (weakness, incomplete paralysis of one or two hind limbs); 3, paraplegia (complete paralysis of two hind limbs); 4, paraplegia with forelimb weakness or paralysis; 5, moribund or death. After the onset of EAE, food and water were provided on the cage floor. Mononuclear cells were prepared from the CNS (brain and spinal cord) of EAE-induced mice and analyzed by flow cytometry.

4.10. T cell adoptive transfer model of colitis

CD4$^+$CD25$^-$CD45RB^{hi} cells from WT and TKO mice were prepared by FACS sorting and adoptively transferred (via i.v. injection) into *Rag1*$-/-$ mice (5×10^5 cells/mouse). Recipient mice were observed daily, and bodyweight was measured weekly. At the end of the

experiment (12wks), all mice were sacrificed, and intestines were removed for hematoxylin and eosin (H&E) staining and histology analysis.

5. ELISA and qRT-PCR

Supernatants of *in vitro* cell cultures were analyzed by ELISA using a commercial assay system (eBioScience). For qRT-PCR, total RNA was isolated using TRI reagent (Molecular Research Center, Inc.) and subjected to cDNA synthesis using RNase H-reverse transcriptase (Invitrogen) and oligo (dT) primers. qRT-PCR was performed in triplicates, using iCycler Sequence Detection System (Bio-Rad) and iQTM SYBR Green Supermix (Bio-Rad). The expression of individual genes was calculated by a standard curve method and normalized to the expression of *Actb*. The gene-specific PCR primers (all for mouse genes) are shown in Supplementary Tables 1–2.

5.1. IB and EMSA

Total cell lysates were prepared and subjected to IB as previously described [47,48].

5.2. RNA-seq analysis

Fresh splenic naïve T cells were isolated from young WT and TKO mice (6–8 week old) and stimulated with plate-coated anti-CD3 (5 μg/ml) and anti-CD28 (1 μg/ml). 18 hrs later, T cells were used for total RNA isolation with Trizol (Invitrogen), and subjected to RNA-seq analysis. RNA sequencing was performed by the Life Science Institute Sequencing and Microarray Facility using an Illumina sequencer. The raw reads were aligned to the mm10 reference genome (build mm10), using Tophat2 RNASeq alignment software. The mapping rate was 70% overall across all the samples in the dataset. HTseq-Count was used to quantify the gene expression counts from Tophat2 alignment files. Differential expression analysis was performed on the count data using R package DESeq2. P-values obtained from multiple binomial tests were adjusted using FDR (BH). Significant genes are defined by a BH corrected p-value of cut-off of 0.05 and fold-change of at least two.

5.3. Real-time quantitative RT-PCR

Total RNA was isolated with TRI reagent (Molecular Research Center) followed by cDNA synthesis with RNase H-reverse transcriptase (Invitrogen) and oligo (dT) primers. Real-time quantitative PCR was done in triplicate with an iCycler Sequence Detection System (Bio-Rad) and iQTM SYBR Green Supermix (Bio-Rad). The expression of individual genes was calculated by relative fold and was normalized to the expression of *Actb*.

5.4. CDK1 and CDK2 activity assay

The spectrometry quantitative detection kit was used for cellular Cdk1/cyclin B-kinase or Cdk2/cyclin A-kinase activity respectively (Genmed Scientifics Inc,GMS50145.1). The Technical background of this kit is that the Cdk1/Cyclin B phosphorylation target sequence is GGGRSPGRRRRK, while Cdk2/Cyclin A phosphorylation target sequence is HHASPRK. Cdk1/Cyclin B or Cdk2/Cyclin A kinase phosphorylated these peptides respectively, and promoted nicotinamide adenine bis nucleotide (NADH) into oxidized nicotinamide adenine bis nucleotide (NAD) by pyruvate kinase (PK) and lactate dehydrogenase (LDH). The changes of peak absorbance (340 nm) were analyzed to quantify the specific activity of Cdk1/cyclin B or Cdk2/cyclin A.

5.5. Chromatin IP (ChIP) assays

ChIP assays were performed with naïve T cells (5×10^6) stimulated for 18 h with plate-coated anti-CD3 (5 μg/ml) and anti-CD28 (1 μg/ml). The cells were fixed with 1% formaldehyde and sonicated as previously described. ChIP-Seq analysis was performed by Active Motif. Seventy-five nucleotide reads generated by Illumina sequencing were mapped to the genome using the BWA algorithm with default settings. Only reads that passed the Illumina purity filter, that aligned with no more than two mismatches, and that mapped uniquely to the genome were used in the subsequent analysis. The heat maps and average profile for RefSeq gene bodies were generated using ngsplot v2.61.

Lysates (from 2×10^7 cells in 3 ml) were subjected to IP with the H4K20me1 antibodies, and the precipitated DNA was then purified by Qiaquick columns (Qiagen) and quantified by QPCR using a pair of primers that amplify the target region of the *Aurka* or *Aurkb* promoter (Supplementary Table 1). The precipitated DNA is presented as percentage of the total input DNA. For histone modification analyses, the DNA bound by modified histone 3 is presented as percentage of total histone 3-bound DNA.

5.6. Statistical analysis

Statistical analysis was performed using Prism software. Two-tailed unpaired t-tests were performed and P values less than 0.05 were considered significant, and the level of significance was indicated as $*P < 0.05$, $**P < 0.01$, $***P < 0.005$. In the animal studies, 4 mice at least are required for each group based on the calculation to achieve a 2.3 fold change (effect size) in two-tailed t -test with 90% power and a significance level of 5%. All statistical tests are justified as appropriate, and data meet the assumptions of the tests. The variance is similar between the groups being statistically compared.

5.7. Data availability

Sequence data that support the findings of this study are available from the authors and have been deposited in the National Center for Biotechnology Information (NCBI) For ChIPseq data, the primary accession code is PRJNA359723.

Author contributions

K.F. and F.W. performed the research, prepared the Figures, and wrote the manuscript; Y.L., L.C., Z.G., Y.Z., J.D., T.H., J.Z., R.L., X. M., H.F. and X.G. contributed experiments; J.J. supervised the work, prepared the Figures and wrote the manuscript.

Competing financial interests

The authors declare no competing financial interests.

Acknowledgements

We thank Dr. Heng-Yu Fan, Dr. Fangwei Wang and Dr. Hai Song for expression plasmid and Tp53flox/flox mice. This study was supported by the National Key Research and Development Program of China (2018YFD0500100), the National Natural Science Foundation of China (81572651/81771675), the Fundamental Research Funds for the Central Universities (2016QN81013), the Thousand Young Talents Plan of China, and the Zhejiang University Special Fund for Fundamental Research.

Appendix A. Supplementary data

Supplementary data related to this article can be found at https://doi.org/10.1016/j.jaut.2018.08.006.

References

[1] P.S. Ohashi, T-cell signalling and autoimmunity: molecular mechanisms of disease, Nat. Rev. Immunol. 2 (2002) 427–438.
[2] A. Skapenko, J. Leipe, P.E. Lipsky, H. Schulze-Koops, The role of the T cell in autoimmune inflammation, Arthritis Res. Ther. 7 (2005) S4.
[3] L. Li, Y. Iwamoto, A. Berezovskaya, V.A. Boussiotis, A pathway regulated by cell cycle inhibitor p27Kip1 and checkpoint inhibitor Smad3 is involved in the induction of T cell tolerance, Nat. Immunol. 7 (2006) 1157–1165.
[4] M. Malumbres, M. Barbacid, Cell cycle, CDKs and cancer: a changing paradigm, Nat. Rev. Canc. 9 (2009) 153–166.
[5] A.J. Levine, p53, the cellular gatekeeper for growth and division, Cell 88 (1997) 323–331.
[6] D.R. Green, M. Schuler, T cell development: some cells get all the breaks, Nat. Immunol. 1 (2000) 15–17.
[7] C. Bertoli, J.M. Skotheim, R.A.M. de Bruin, Control of cell cycle transcription during G1 and S phases, Nat. Rev. Mol. Cell Biol. 14 (2013) 518–528.
[8] J. Song, S. Salek-Ardakani, T. So, M. Croft, The kinases aurora B and mTOR regulate the G1-S cell cycle progression of T lymphocytes, Nat. Immunol. 8 (2007) 64–73.
[9] H. Kiyokawa, R.D. Kineman, K.O. Manova-Todorova, V.C. Soares, E.S. Hoffman, M. Ono, et al., Enhanced growth of mice lacking the cyclin-dependent kinase inhibitor function of p27Kip1, Cell 85 (1996) 721–732.
[10] K. Nakayama, N. Ishida, M. Shirane, A. Inomata, T. Inoue, N. Shishido, et al., Mice lacking p27Kip1 display increased body size, multiple organ hyperplasia, retinal dysplasia, and pituitary tumors, Cell 85 (1996) 707–720.
[11] M.L. Fero, M. Rivkin, M. Tasch, P. Porter, C.E. Carow, E. Firpo, et al., A syndrome of multiorgan hyperplasia with features of gigantism, tumorigenesis, and female sterility in p27Kip1-deficient mice, Cell 85 (1996) 733–744.
[12] D. Balomenos, J. Martin-Caballero, M.I. Garcia, I. Prieto, J.M. Flores, M. Serrano, et al., The cell cycle inhibitor p21 controls T-cell proliferation and sex-linked lupus development, Nat. Med. 6 (2000) 171–176.
[13] H.S. Madapura, D. Salamon, K.G. Wiman, S. Lain, G. Klein, E. Klein, et al., p53 contributes to T cell homeostasis through the induction of pro-apoptotic SAP, Cell Cycle 11 (2012) 4563–4569.
[14] Y.-C. Liu, J. Penninger, M. Karin, Immunity by ubiquitylation: a reversible process of modification, Nat. Rev. Immunol. 5 (2005) 941–952.
[15] F. Huang, H. Gu, Negative regulation of lymphocyte development and function by the Cbl family of proteins, Immunol. Rev. 224 (2008) 229–238.
[16] M. Chang, W. Jin, J.-H. Chang, Y. Xiao, G.C. Brittain, J. Yu, et al., The ubiquitin ligase Peli1 negatively regulates T cell activation and prevents autoimmunity, Nat. Immunol. 12 (2011) 1002–1009.
[17] N. Anandasabapathy, G.S. Ford, D. Bloom, C. Holness, V. Paragas, C. Seroogy, et al., GRAIL: an E3 ubiquitin ligase that inhibits cytokine gene transcription is expressed in anergic CD4+ T cells, Immunity 18 (2003) 535–547.
[18] H. Hu, H. Wang, Y. Xiao, J. Jin, J.-H. Chang, Q. Zou, et al., Otud7b facilitates T cell activation and inflammatory responses by regulating Zap70 ubiquitination, J. Exp. Med. 213 (2016) 399–414.
[19] N. Shembade, N.S. Harhaj, K. Parvatiyar, N.G. Copeland, N.A. Jenkins, L.E. Matesic, et al., The E3 ligase Itch negatively regulates inflammatory signaling pathways by controlling the function of the ubiquitin-editing enzyme A20, Nat. Immunol. 9 (2008) 254–262.
[20] Z. Hao, Y. Sheng, G.S. Duncan, W.Y. Li, C. Dominguez, J. Sylvester, et al., K48-linked KLF4 ubiquitination by E3 ligase Mule controls T-cell proliferation and cell cycle progression, Nat. Commun. 8 (2017) 14003.
[21] Z. Guo, Q. Kong, C. Liu, S. Zhang, L. Zou, F. Yan, et al., DCAF1 controls T-cell function via p53-dependent and -independent mechanisms, Nat. Commun. 7 (2016) 10307.
[22] H. Oda, M.R. Hübner, D.B. Beck, M. Vermeulen, J. Hurwitz, D.L. Spector, et al., Regulation of the histone H4 monomethylase PR-set7 by CRL4Cdt2-mediated PCNA-dependent degradation during DNA damage, Mol. Cell 40 (2010) 364–376.
[23] K. Terai, T. Abbas, A.A. Jazaeri, A. Dutta, CRL4Cdt2 E3 ubiquitin ligase monoubiquitinates PCNA to promote translesion DNA synthesis, Mol. Cell 37 (2010) 143–149.
[24] T. Abbas, U. Sivaprasad, K. Terai, V. Amador, M. Pagano, A. Dutta, PCNA-dependent regulation of p21 ubiquitylation and degradation via the CRL4Cdt2 ubiquitin ligase complex, Genes Dev. 22 (2008) 2496–2506.
[25] M.K. Diril, C.K. Ratnacaram, V.C. Padmakumar, T. Du, M. Wasser, V. Coppola, et al., Cyclin-dependent kinase 1 (Cdk1) is essential for cell division and suppression of DNA re-replication but not for liver regeneration, Proc. Natl. Acad. Sci. Unit. States Am. 109 (2012) 3826–3831.
[26] A. Heim, B. Rymarczyk, T.U. Mayer, Regulation of cell division, in: F. Pelegri, M. Danilchik, A. Sutherland (Eds.), Vertebrate Development: Maternal to Zygotic Control, Springer International Publishing, Cham, 2017, pp. 83–116.
[27] Moriggl R, Topham DJ, Teglund S, Sexl V, McKay C, Wang D et al. Stat5 is required for IL-2-induced cell cycle progression of peripheral T cells. Immunity;10:249-259.
[28] L.-H. Zhang, J.O. Liu, A. Sanglifehrin, A novel cyclophilin-binding immunosuppressant, inhibits IL-2-dependent T cell proliferation at the G_1 phase of the cell cycle, J. Immunol. 166 (2001) 5611–5618.
[29] C.F. Arias, A. Ballesteros-Tato, M.I. García, J. Martín-Caballero, J.M. Flores, -A.C. Martínez, et al., $p21^{CIP1/WAF1}$ controls proliferation of activated/memory T cells and affects homeostasis and memory T cell responses, J. Immunol. 178 (2007) 2296–2306.
[30] H. Nishitani, Y. Shiomi, H. Iida, M. Michishita, T. Takami, T. Tsurimoto, CDK inhibitor p21 is degraded by a proliferating cell nuclear antigen-coupled cul4-DDB1Cdt2 Pathway during S Phase and after UV irradiation, J. Biol. Chem. 283 (2008) 29045–29052.
[31] J. Fu, M. Bian, Q. Jiang, C. Zhang, Roles of aurora kinases in mitosis and tumorigenesis, Mol. Canc. Res. 5 (2007) 1–10.
[32] P.A. Coelho, J. Queiroz-Machado, A.M. Carmo, S. Moutinho-Pereira, H. Maiato, C.E. Sunkel, Dual role of topoisomerase II in centromere resolution and aurora B activity, PLoS Biol. 6 (2008) e207.
[33] X. Guo, X. Wang, Z. Wang, S. Banerjee, J. Yang, L. Huang, et al., Site-specific proteasome phosphorylation controls cell proliferation and tumorigenesis, Nat. Cell Biol. 18 (2016) 202–212.
[34] T.A. Potapova, J.R. Daum, B.D. Pittman, J.R. Hudson, T.N. Jones, D.L. Satinover, et al., The reversibility of mitotic exit in vertebrate cells, Nature 440 (2006) 954.
[35] C.L. Sansam, J.L. Shepard, K. Lai, A. Ianari, P.S. Danielian, A. Amsterdam, et al., DTL/CDT2 is essential for both CDT1 regulation and the early G2/M checkpoint, Genes Dev. 20 (2006) 3117–3129.
[36] C.G. Havens, J.C. Walter, Mechanism of CRL4Cdt2, a PCNA-dependent E3 ubiquitin ligase, Genes Dev. 25 (2011) 1568–1582.
[37] F. Bassermann, R. Eichner, M. Pagano, The ubiquitin proteasome system — implications for cell cycle control and the targeted treatment of cancer, Biochim. Biophys. Acta (BBA) Mol. Cell Res. 1843 (2014) 150–162.
[38] R. Moriggl, D.J. Topham, S. Teglund, V. Sexl, C. McKay, D. Wang, et al., Stat5 is required for IL-2-induced cell cycle progression of peripheral T cells, Immunity 10 (1999) 249–259.
[39] M. Iacobelli, F. Rohwer, P. Shanahan, J.A. Quiroz, K.L. McGuire, IL-2-Mediated cell cycle progression and inhibition of apoptosis does not require NF-κb or activating Protein-1 activation in primary human T cells, J. Immunol. 162 (1999) 3308–3315.
[40] Y. Rochman, R. Spolski, W.J. Leonard, New insights into the regulation of T cells by [gamma]c family cytokines, Nat. Rev. Immunol. 9 (2009) 480–490.
[41] A. Jatzek, M. Marie Tejera, E.H. Plisch, M.L. Fero, M. Suresh, T-cell intrinsic and extrinsic mechanisms of p27Kip1 in the regulation of CD8 T-cell memory, Immunol. Cell Biol. 91 (2013) 120–129.
[42] A. Jatzek, M.M. Tejera, A. Singh, J.A. Sullivan, E.H. Plisch, M. Suresh, $p27^{Kip1}$ negatively regulates the magnitude and persistence of CD4 T cell memory, J. Immunol. 189 (2012) 5119–5128.
[43] R. Wang, P. Dillon Christopher, Z. Shi Lewis, S. Milasta, R. Carter, D. Finkelstein, et al., The transcription factor myc controls metabolic Reprogramming upon T Lymphocyte activation, Immunity 35 (2011) 871–882.
[44] S.K. Radhakrishnan, C.S. Lee, P. Young, A. Beskow, J.Y. Chan, R.J. Deshaies, Transcription factor Nrf1 mediates the proteasome recovery pathway after proteasome inhibition in mammalian cells, Mol. Cell 38 (2010) 17–28.
[45] X. Wang, L. Huang, Identifying dynamic interactors of protein complexes by quantitative mass spectrometry, Mol. Cell. Proteomics 7 (2008) 46–57.
[46] X. Wang, C.-F. Chen, P.R. Baker, P-l Chen, P. Kaiser, L. Huang, Mass spectrometric characterization of the affinity-purified human 26S proteasome complex, Biochemistry 46 (2007) 3553–3565.
[47] W.W. Reiley, W. Jin, A.J. Lee, A. Wright, X. Wu, E.F. Tewalt, et al., Deubiquitinating enzyme CYLD negatively regulates the ubiquitin-dependent kinase Tak1 and prevents abnormal T cell responses, J. Exp. Med. 204 (2007) 1475–1485.
[48] M.R. Waterfield, M. Zhang, L.P. Norman, S.-C. Sun, NF-κB1/p105 regulates lipopolysaccharide-stimulated MAP kinase signaling by governing the stability and function of the Tpl2 kinase, Mol. Cell 11 (2003) 685–694.